

Characterisation and Corrosion Performance of Multilayer Nano Nickel Coatings on AZ31 Magnesium Alloy

M. Tafazoly*, M. Monirvaghefi, M. Salehi, A. Saatchi, F. Tabatabaei, M. M. Verdian

Department of Materials Engineering, Isfahan University of Technology (IUT), Isfahan, I. R. Iran

(*) Corresponding author: mah_tafazoly@yahoo.com
(Received: 25 Nov. 2011 and Accepted: 17 March 2012)

Abstract:

Ni-P and Ni layers multilayer coatings were applied to AZ31 magnesium alloy utilizing electroless and electrodeposition procedures. The aim of the project was to decrease cracks and increase corrosion resistance of the coatings. In order to compare the coatings, the effect of single layer electroless Ni-P coatings with different thicknesses was also investigated. The microstructure and phase composition of the coatings were investigated by scanning electron microscopy (SEM) and X-ray diffraction (XRD) analysis. The results showed that increase in the thickness of the single layer coatings was not an effective solution to inhibit the reaction of magnesium with plating bath during electroless process. In this regard, magnesium was detected on the surface of the single layer coatings. The application of a thin electroplated Ni layer between two electroless layers could inhibit the reaction of magnesium with plating bath during electroless process, which resulted in improving the corrosion resistance of the coatings.

Keywords: Magnesium alloys, Electroless Ni-P, Electrodeposition, Corrosion, Multilayer coatings.

1. INTRODUCTION

Magnesium is the lightest constructional metal which has a density of 1.74 gr cm^{-3} [1]. In this regard, magnesium is 35% and 78% lighter than aluminium and steel, respectively. Magnesium and its alloys are promising due to their high specific strength and stiffness, good ductility and high damping characteristics [1-3]. Therefore, magnesium alloys are used in a wide variety of applications such as automotive and aerospace industries due to their attractive properties [1].

AZ31 is a commercially well-known magnesium alloy. The microstructure of this alloy consists of two different phases; eutectic α -phase as a matrix, and small amounts of β - phase [4]. This alloy offers good physical and mechanical properties at room temperature and it is widely used in industry [4]. Although AZ31 and other magnesium alloys

promise great advantages, but the inherently poor corrosion resistance of these alloys is the main limitation when they are used in industry [4,5]. Magnesium is a very electrochemically reactive element in corrosion environments [6]. The standard electrode potential for magnesium at 25°C is -2.3V , while this value for iron is -0.44 in seawater [5]. In addition, AZ31 magnesium alloy has a critical corrosion problem because the alloy contains small amounts of β phase in addition to α phase [4]. Since α and β phases exhibit different corrosion potentials in corrosion environments, so, a microgalvanic couple is created between these phases which accelerates the corrosion rate [4]. On the other hand, the formability of AZ31 alloy is poor at room temperature [7]. In order to improve formability, AZ31 is warmly formed at about 225°C [7]. The operation at this temperature affects the surface appearance of alloy which is not acceptable

in many applications [7,8]. Therefore, the surface appearance and corrosion resistance of AZ31 magnesium alloy should be improved.

The application of an electroless nickel-phosphorus coating on the surface can be an effective solution for simultaneous improvement in surface appearance and corrosion resistance. Electroless nickel coatings summarised as EN have found wide industrial applications due to their excellent mechanical, physical, electrical, as well as corrosion and wear resistant properties. The application of EN coatings is a suitable method for surface modification of magnesium and its alloys [9-12]. Electroless Ni plating is an autocatalytic chemical reduction process in which the reducing agent is oxidised and Ni^{2+} ions are deposited (reduced) on the substrate surface without using an electric current [10]. Once the first layer of Ni is deposited, it acts as a catalyst for the upper layers [10].

The EN deposition process starts only on the catalytic surface; and it involves diffusion of chemicals to the deposited surface and by-products away from the surface [13]. Hydrogen is one of the by-products evolved from the deposit surface during the electroless plating process. So, in electroless plating process, a large amount of H_2 gas bubbles are produced, and that may lead to the formation of pores in the coatings. In addition, magnesium alloys can easily react with the plating bath. This phenomenon can increase open pores in the electroless Ni layer. When open pores are present in the electroless coatings, the electrolyte can easily penetrate along them and finds direct paths to the substrate [13].

Since nickel is electrochemically nobler than magnesium, so, a galvanic couple is created at the substrate/coating interface which accelerates the corrosion of the substrate. As a result, the substrate will be severely corroded. Thus, porosity plays a crucial role in EN coating on magnesium alloys and can influence the corrosion behaviour and service lifetime of the electroless nickel plated magnesium [14].

Furthermore, the coating thickness has a strong effect on the porosity. A dramatic reduction in porosity was found for deposits thicker than $12\mu\text{m}$, but, the increase in the thickness of the electroless

coating is not effective to close the open pores [13]. The application of a multilayer electroless coating may be effective to close the open pores. In this regard, Changdong *et al* [15]. investigated a multilayer Ni-P (low phosphorus)/Ni/Ni-P (high phosphorus) coating on steel substrate. They reported that multilayer coatings exhibit better corrosion resistance in comparison to single layer coatings [15]. The multilayer coatings can be developed on AZ31 substrate to produce corrosion resistant coatings. However, the electroless process on magnesium alloys is not as easy as that on steel and aluminium, because magnesium is very reactive and can easily react with the plating bath. To decrease the reaction of magnesium with plating bath, in the pre-cleaning step MgF_2 passive film is created on the surface of magnesium substrate to reduce the active surface of base alloy, it's an uncontinuous film and electroless mechanism starts from the magnesium surface without passive film. Therefore, the usual electroless processes on steel and aluminium can not be utilised for magnesium substrates.

In this study, the multilayer coatings consisting of Ni-P and Ni layers were deposited on AZ31 magnesium alloy. In this regard, SLOTONIP 70A bath which is a commercial and economical bath for electroless process was developed for AZ31 substrate. The phosphorus content of electroless layers was constant, and the main purpose was to improve the corrosion resistance of the coatings. The microstructure, surface morphology and corrosion resistance of the coatings were also investigated.

2. EXPERIMENTAL PROCEDURES

AZ31 (Mg-3.2Al-1.1Zn-0.5Mn-0.05Si-0.04Ca-0.01Cu, wt-%) rolled sheets with the dimensions of $20\text{mm}\times 20\text{mm}\times 3\text{mm}$ were used as the substrate material. The substrates were wet ground up to 600 grit SiC paper and then were polished using a diamond wheel. After that, the coupons were blasted with SiO_2 grits to a surface roughness (Ra) of $3.6\mu\text{m}$. Then, all the samples were subjected to the following pre-treatment: ultrasonic cleaning in absolute ethanol at 25°C for 5 min; alkaline cleaning

in NaOH (45g/L) at 25°C for 10 min; acid pickling in HNO₃ (80 vol.%) at 25°C for 60s and activation in (40vol.%) HF at 25°C for 10 min. The samples were transferred to the plating bath immediately after the pre-cleaning steps.

The commercial SLOTONIP 70 A electroless Nickel bath, was used for the deposition of nickel-phosphorus coatings. The bath composition is given in Table 1. The treatment was performed at pH 6.4 and temperature 82°C at a deposition rate of 20µm/h. The bath was stirred with a speed of 400 rpm, using a magnetic agitation system and a 2.5 cm long and 7.5mm diameter PTFE coated magnet. The coated samples were removed from the bath, washed with water and acetone and then air-dried.

In the first stage of the coating process, single layer coatings with different thicknesses were deposited. The details of the coatings and abbreviations used are given in Table 2. In the second stage, 4µm thick electroplated Ni coating were applied to 20thEN sample from a bath containing nickel sulphate, nickel chloride and boric (Table 3) at a pH of 5.0 and a temperature of 25 °C. The direct current was

2.6 A dm⁻². The coating prepared in this stage was referred to as EN/nc. In the third stage, another 20µm thick electroless layer was deposited on EN/nc sample. The bath composition and operating conditions used in this stage were similar to those used in the first stage. The coating prepared in this stage was referred to as EN/nc/EN.

The coatings were analysed by X-ray diffractometry (XRD, Philips X'Pert-MPD) using Cu-Kα radiation (1.54056 Å) generated at 40 kV and 30 mA. For microstructural and surface morphology examination, a scanning electron microscope (SEM, Philips XL30) operated at 20 kV equipped with an energy dispersive spectroscope (EDS) for microanalysis was used.

Electrochemical measurements were performed using a PARSTAT 2273 potentiostat which was controlled by a computer and supported by software. Tafel polarisation experiments were carried out in a 3.5 wt.% NaCl solution using a classic three-electrode cell. The platinum plate (Pt) was the counter electrode and a Calomel electrode was used as a reference electrode. The corrosion

Table 1: The chemical composition of electroless bath.

Agent	Concentration
Nickel	7 g/L
Reducer, SH	45 mL/L
Stabiliser	7 mL/L

Table 2: The details of single layer coatings.

Thickness(µm)	Abbreviation
7µm	7thEN
10µm	10thEN
15µm	15thEN
20µm	20thEN

Table 3: The chemical composition of electrodeposition bath.

Agent	Concentration
NiSO ₄ .6H ₂ O	250-300 g/L
NiCl ₂ .6H ₂ O	30-40 g/L
H ₃ BO ₃	30-45 g/L

Table 4: Corrosion parameters estimated from the polarisation curves of substrate and single layer coatings

Specimen	$E_{\text{corr}}, V_{\text{SCE}}$	$i_{\text{corr}}, \mu\text{A cm}^{-2}$
Substrate	-1.53	800
7thEN	-1.36	650
10thEN	-1.24	600
15thEN	-1.23	65
20thEN	-1.27	34

Table 5: Corrosion parameters estimated from the polarisation curves of single and multilayer coatings

Specimen	$E_{\text{corr}}, V_{\text{SCE}}$	$i_{\text{corr}}, \mu\text{A cm}^{-2}$
20thEN	-1.27	34
EN/nc	-1.29	80
EN/nc/EN	-1.17	0.6

potential (E_{corr}) and corrosion current density (i_{corr}) were extracted from E-logI curves using Tafel extrapolation method.

3. RESULTS AND DISCUSSION

3.1. X-ray diffraction analysis of the coatings

The X-ray diffractograms of coatings are shown in Figure 1. A wide hump and a single Ni peak appear in the X-ray diffractogram of single layer indicating that the single layer coating has an amorphous/nanocrystalline structure [16]. The grain size of electroless layers was determined via Scherrer equation [17]. It is worth noting that low phosphorous EN coatings are nano-crystalline [9,12,13]. and using the Scherrer formula is only for determining the grain size of the EN layer.

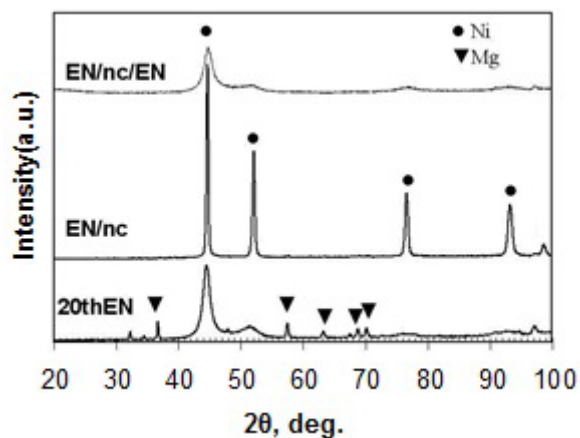


Figure 1: The XRD patterns of single and multilayer coatings.

In this case, the average grain size of the single EN layer was about 22 nm. It has been reported that amorphous and/or nanocrystalline phases can be obtained in EN coatings depending on the phosphorus content of EN coatings [18-20]. In addition, Mg peaks can be seen in the XRD pattern of single layer coatings. It is probably due to the presence of Mg in the coating structure. It seems that this feature arises as a result of the reaction of magnesium with plating bath. In this regard, magnesium has been detected in electroless Ni coatings deposited on magnesium alloys [10]. In

contrast, no Mg peaks can be observed in the XRD patterns of EN/nc and EN/nc/EN samples. The EN/nc/EN coating also has a nanocrystalline structure with the average grain size of about 42 nm.

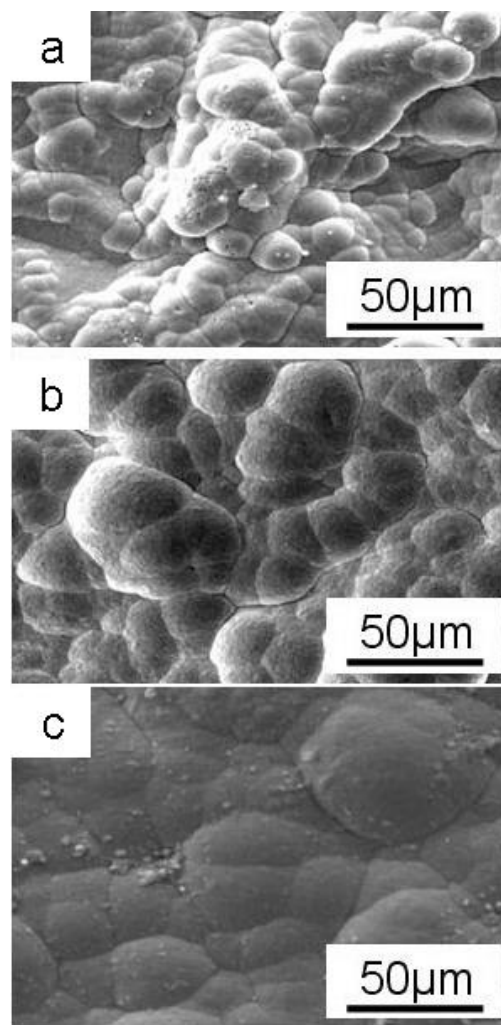


Figure 2: The morphology of a) 20th EN, b) EN/nc and c) EN/nc/EN samples.

3.2. Microstructure of the coatings

Figure 2 shows the morphology of coatings. It can be seen that single electroless Ni coating has a ‘cauliflower-like’ structure (Figure 2a), including a few micro cracks marked in the figure. These defects can affect the good properties of the coating. If there was a difference between the thermal expansion coefficients of the coating and the substrate, the coating might fail due to the cracking caused by

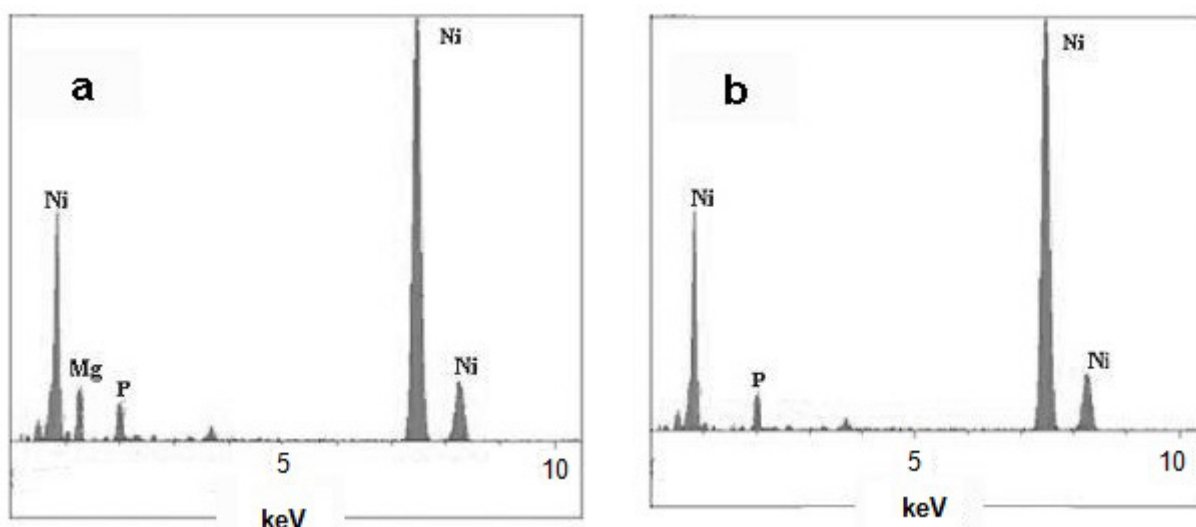


Figure 3: EDS X-ray spectrums from a) 20th EN and b) EN/nc/EN samples.

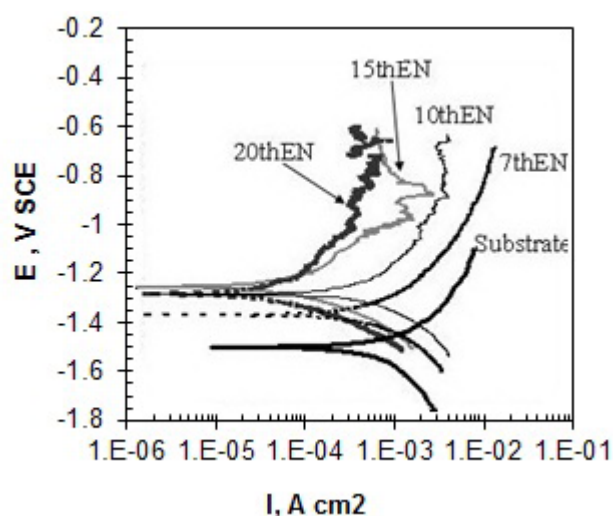


Figure 4: The potentiodynamic polarisation curves for the substrate and single layer coatings with different thicknesses.

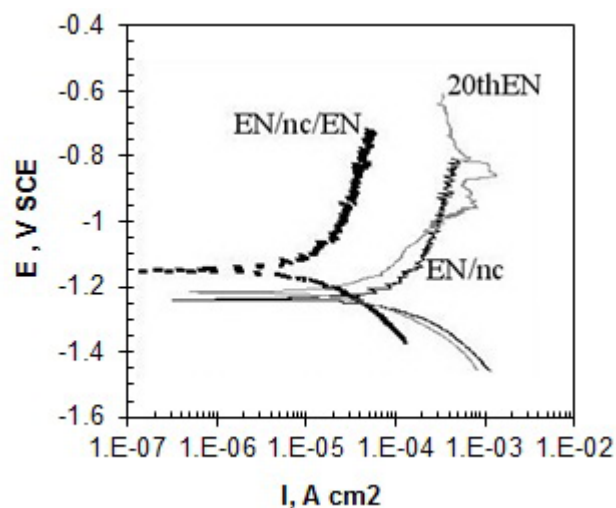


Figure 5: The potentiodynamic polarisation curves of 20th EN, EN/nc and EN/nc/EN samples.

residual thermal stresses [21]. The residual thermal stresses created at the substrate-coating interface cause initiation and propagation of cracks which may eventually lead to failure [21]. However, AZ31 has approximately high thermal expansion coefficients of about $25.2 \times 10^{-6} \text{ K}^{-1}$, and unlike many conventional coating methods, EN coatings have a wide range of thermal expansion coefficients depending on the phosphorus content [21]. The coefficients of thermal expansion of EN coatings vary from $22.3 \times 10^{-6} \text{ K}^{-1}$ for low phosphorus (3

wt.%) coating to $11.1 \times 10^{-6} \text{ K}^{-1}$ for high phosphorus (11 wt.%) coating [21]. So, micro cracks may be created due to the difference between the thermal expansion coefficients of the substrate and coating. The low-phosphorus coating has fewer micro cracks compared to high and medium-phosphorus coatings [21]., so, the low-phosphorus coating was used for electroless plating of AZ31.

The morphology of the EN/nc sample could be seen in Figure 2.b. As shown in this Figure, this coating has the 'cauliflower-like' structure like EN coating.

But, EN/nc microstructure exhibits no microcracks due to the similarity in thermal expansion coefficients of low-phosphorus electroless and Ni electroplated coating. As shown in Figure 2.c, the microstructure of EN/nc/EN sample exhibits a smoother surface. In addition, no microcracks exist in this sample. Figure 3 shows the EDS X-ray spectrums from 20th EN and EN/nc/EN samples. As shown in Figure 3.a, 4 wt.% of magnesium was detected on the surface of the 20th EN sample, due to presence of magnesium on the surface. So, increasing the thickness of single layers is not an effective way to inhibit the reaction of magnesium with bath. According to the Figure 3.b, magnesium was not detected on the surface of EN/nc/EN multilayer coating. It seems that the application of a thin electroplated Ni layer between two electroless layers could inhibit the reaction of magnesium with plating bath during electroless process. These results are in agreement with those obtained by XRD (Figure 1).

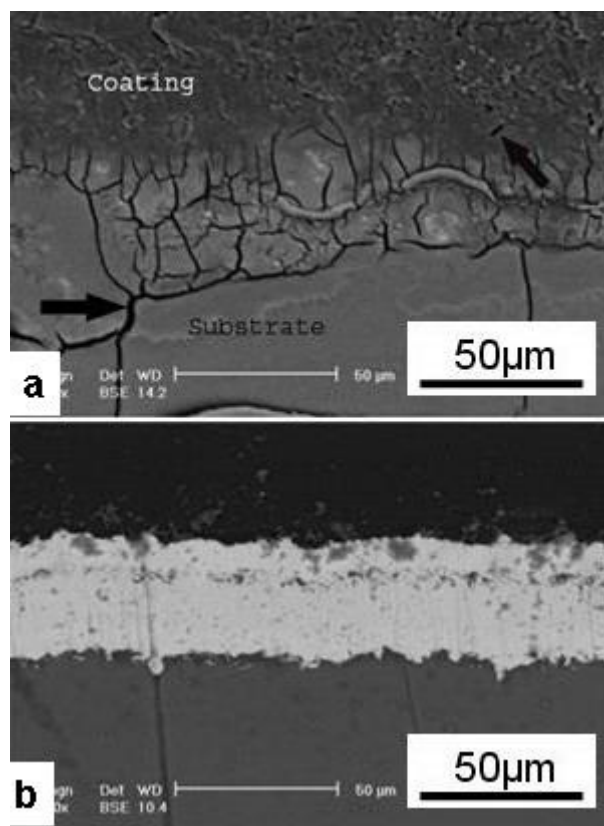


Figure 6: SEM micrographs from cross-section of a) 20th EN and b) EN/nc/EN samples after corrosion tests.

3.3. Corrosion resistance measurements

Figure 4 shows the potentiodynamic polarisation curves for the substrate and single layer coatings with different thicknesses. The values of corrosion current density (i_{corr}) and corrosion potential (E_{corr}) were estimated from the polarisation curves using Tafel extrapolation method as summarised in Table 4. From Table 4, it can be seen that E_{corr} of the single layer coatings are less negative than that of the substrate and positively shift as thickness of coatings increased. It can be due to decrease of the porosity [13]. I_{corr} also decreases as the coating thickness increased. It has been reported that the increase in the thickness of the electroless coating may be effective to close the open pores and consequent improvement in corrosion behaviour [13].

The potentiodynamic polarisation curves of 20th EN, EN/nc and EN/nc/EN samples are shown in Figure 5. The respective i_{corr} and E_{corr} values are given in Table 5. It can be seen that the corrosion E_{corr} of multilayer (EN/nc/EN) sample is higher than that of the other samples. In addition, i_{corr} for this sample this sample is much lower than that for single and double layer coatings. It seems that open pores have been completely plugged in EN/nc/EN sample.

SEM micrographs from cross-section of 20th EN and EN/nc/EN coatings after corrosion tests are shown in Figure 6. In the case of 20th EN coating, the substrate seems to be severely attacked (Figure 6a). In this figure, the cracks in the substrate have been shown by black arrows. The cracks seem to be the results of intergranular corrosion of substrate which is catastrophic [21]. It has been reported that magnesium alloys are susceptible to intergranular corrosion in chloride media [5,22]. In the case of EN/nc/EN coatings (Figure 5.b), the substrate has not been corroded and no attack can be detected through the coating and along the coating/substrate interface. This indicates that the multilayer layer could prevent the penetration of electrolyte through the coating.

4. CONCLUSIONS

Based on the results from this experiment, the following conclusions may be drawn:

1. Ni-P and Ni multilayer coatings were deposited on AZ31 magnesium alloy utilizing electroless and electrodeposition techniques. The results showed that these coatings had nanocrystalline structure.
2. In the case of single layer electroless coatings, increasing the thickness of the coatings was not an effective solution to inhibit the reaction of magnesium with plating bath during electroless process. In this regard, magnesium was detected on the surface of the single layer coatings.
3. The application of a thin electroplated Ni layer between two electroless layers could inhibit the reaction of magnesium with plating bath during electroless process, which resulted in improvement of corrosion resistance of the coatings.

REFERENCES

1. M. K. Kulekci: Int J Adv Manuf Technol., Vol. 39, (2008), pp. 851–865.
2. D. Eliezer and E. Aghion: Adv. Perf. Mat., Vol. 5, (1998), pp. 201–212.
3. F.H. Froes, D. Eliezer and E. Aghion: J. MIN. MET. MAT. S., Vol. 50, No. 9, (1998), pp. 30-34.
4. S. A. Salman, R. Ichino and M. Okido: Int. J. Corros., Vol. 2010, (2010), pp. 7.
5. E. Ghali and W. Dietzel: J. Mat. Eng. Perf., Vol. 13, No. 1, (2003), pp. 7-23.
6. T. Ishizaki and I. Shigematsu: Surf. Coat. Technol., Vol. 203, (2009), pp. 2288-2290.
7. H. Huo and Y.Li: Corros. Sci., Vol. 46, (2004), pp. 1467–1477.
8. K. Abu-Farha and M. K. Khraisheh: J. Mat. Eng. Perf., Vol. 16, No. 2, (2007), pp. 192-199.
9. J.A. Del Valle, M.T. Perez-Prado and O.A. Ruano: Metall. Mater. Trans. A, Vol. 36A, (2005), pp. 1427-1438.
10. KH.M. Shartal and G.J. Kipouros: Metall. Mater. Trans. A, Vol. 40, No. 2, (2009), pp. 208-222.
11. K.G. Keong, W. Sha and S. Malinov: Surf. Coat. Technol., Vol. 168, (2003), pp. 263–274.
12. M. Yan, H.G. Ying and T.Y. Ma: Surf. Coat. Technol., Vol. 202, (2008), pp. 5909–5913.
13. J.Li, Y. Tian, Z.Huang and X. Zhang: App. Surf. Sci., Vol. 252, (2006), pp. 2839–2846.
14. M.Araghi and M.H. Paydar: Materials and Design, Vol. 31, (2010), pp. 3095–3099.
15. Ch.Gua and J. Liana: Surf. Coat. Technol., Vol. 197, (2005), pp. 61– 67.
16. M. Palaniappa and S. K. Seshadri: J. Mater. Sci., Vol. 42, (2007), pp. 6600-6606.
17. B.D. Cullity and S.R. Stock: 'Elements of X-Ray Diffraction', 3rd edn, 351; 2001, Englewood. Cliffs, New Jersey, Prentice Hall.
18. D. Barker: Trans Inst. Metal Finishing, Vol. 71, No. 3, (1993), pp. 121-125.
19. Y.Z. Zhang and M. Yao: Trans Inst. Metal Finishing, Vol. 77, No. 2, (1999), pp. 78-83.
20. Y.Z. Zhang, Y.Y. Wu and M. Yao: J. Mater. Sci. Lett., Vol. 17, No. 1, (1998), pp. 37-40.
21. R.N. Duncan: Plating and Surf. Finish., Vol. 83, (1996), pp. 65-83.
22. G. Song, A. Atrens, X. Wu and B. Zhang: Corros. Sci., Vol. 40, No. 10, (1998), pp. 1769-1791.

